

# Modeling Methods and Simulation Analysis of Radial Tire with Different Tread Patterns

Yongqiang Li, Congzhen Liu \*, Yunfen Sun, Yalong Li, Chengwei Xu and Mengyu Xie

School of Transportation and Vehicle Engineering, Shandong University of Technology, 255049, Zhangdian district, Zibo city, Shandong province, China.

\*Corresponding author email id: lcz200811@163.com

Date of publication (dd/mm/yyyy): 06/02/2020

**Abstract** – This study focus on the modeling methods of radial tires with different tread patterns and conducts simulation analysis. Considering the material nonlinearity and geometric nonlinearity of tire, Hypermesh and ABAQUS finite element software were used to study the modeling method. Under the standard pressure, two tire models are simulated under static load. The vertical stress distribution of contact patch and the relationship between load and subsidence were obtained. Moreover, the influence of tread patterns and load on contact patch were analyzed. The results show that the relationship between load and subsidence is approximately a linear function. With the load increases, the peak stress location shifts from the center of crown to the shoulders. The peak stress of tires with complex tread patterns are greater than that with only longitudinal grooves. With the increase of the load, the grounding area of both types of tread patterns tires gradually increases, and the grounding area of complex tread patterns tire is small than that of longitudinal groove tire. The research results provide a finite element simulation reference for the further optimization of tire design.

**Keywords** – Radial Tire, Tread Patterns, Modeling Method, Simulation Analysis.

## I. INTRODUCTION

Tires are components that directly contact with the ground. All the force between the vehicle and the ground is transmitted through the tires. Therefore, the performance of tires is closely related to the driving and safety performance of vehicles. Tire rubber is a hyperelastic constitutive model material, and the stress-strain relationship is nonlinear. The contact between tire, ground and rim is also a typical non-linear contact problem, with large deformation in the process [1]. Traditional tire design is mainly based on theoretical design under the mode of experience and semi-experience. Which is heavy in workload, long in time consumption and low in accuracy, and is difficult to meet the needs of rapid development of tire industry. With the maturity of finite element simulation technology, finite element method has been widely used in tire mechanics research [2].

For the modeling and analysis of radial tire, Akbar m. Farahani [3] et al established the tire and linear elastic rim models composed of the new hooker model, and verified the tire modes through experiments. Koehne, S.H. [4] et al. developed a tire contact stress testbed, simulated tire contact stress with finite element method, and carried out mechanical interpretation. Ha Si-ba-gen [5] et al. simplified the design of the main parts of the tire and analyzed the tire stiffness under different road conditions. P.S. Pillai [6] et al. analyzed the tire contact patch by test method, and calculated the empirical formula of tire grounding area according to tire deformation and sidewall size parameters. Haibo Huang [7] et al. established a longitudinal groove tire model to study the influence of various parameters on the asymmetric index of ground pressure distribution under tire rolling condition. Hairong Chen [8] et al. studied the establishment of complex pattern radial tire model, and compared the simulation time with simple pattern tire to verify the accuracy of the model. Huilin Du [9] et al. established a simplified tire model to study the contact stress between tire and road surface under different air pressures.

Scholars at home and abroad have made more comprehensive research on modeling and analysis of smooth tire

or single pattern tire, while relatively less research and detailed simulation and comparative analysis on modeling process of common longitudinal groove tire and complex tread patterns tire.

In this paper, the modeling methods of longitudinal groove tire and complex tread patterns tire are studied by finite element software. Under the standard pressure, the static load conditions of two kinds of tire models are simulated, and the correctness of the models is verified by experiments. The relationship between load and subsidence, tire vertical stress distribution, and the influence of pattern and load on grounding area were studied. The research conclusion can provide reference for the next step of tire design.

## II. EXPERIMENTS

### A. Test Instrument

In this paper, the static load test equipment for tires is CSS-88100 static load testing machine, the product of Changchun Testing Machine Research Institute. Used to test the size of the load and the contact patch of the tire. Laser level instrument, Products of Nantong Yagu Tools Company, Ensure that the radial force loading angle of the rigid platform is 90°. Air pump with air pressure detection, Ensure the test tire pressure is stable. Steel ruler for measuring radial deformation of tires.

### B. Method of Test

According to the standard " Method of automobile tire static contact pressure distribution " to determine the test method. The test environment temperature is 18 ~ 36°C, and the humidity is 45%. The test tire is shown in Fig. 1.

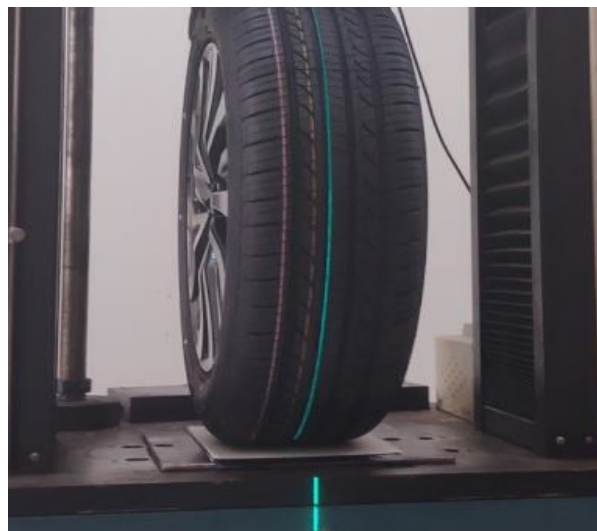


Fig. 1. The test tire.

### Experimental Steps:

1. Install the tire to be tested on the standard rim, inflate to the standard air pressure ( $\pm 5$  kPa), and measure the air pressure of the tire after 24 hours in the laboratory. If the air pressure is insufficient, continue to pressurize and park for 15min before testing.
2. Clean up the dirt on the tire surface and other pollutants affecting the test, trim the tire lanugo hair and other rubber residues formed in the process of vulcanizing the tire, and mark 6 test points on the tire sidewall after

inflation.

3. Loading tests are carried out on six points to be tested in sequence on a static loading testing machine, so as to ensure the accuracy of data and obtain the contact patch and radial deformation of tires under different loads.

### III. FINITE ELEMENT MODEL OF TIRE

#### A. Material Model

The composition of tire is relatively complex, which consists of tread, carcass, bead, belt, tire apex and other components. Different parts are characterized by different material properties respectively [10]. The carcass and belt are rubber-cord composite materials, which are simulated by Rebar material model. Rebar layer is usually used to simulate uniaxial reinforcement in shell, membrane and surface unit. Compared with tire matrix material, Rebar layer has stronger material rigidity, and its elastic characteristics can be used for the characteristics of steel wire layer material (except yield and ultimate load calculation). Rebar material model properties are shown in Table 1. Yeoh material model is used to simulate rubber materials such as tread and carcass. The constitutive equation of strain energy of Yeoh model is [11]:

$$W = C_{10} (I_1 - 3) + C_{20} (I_1 - 3)^2 + C_{30} (I_1 - 3)^3 \quad (1)$$

Where  $W$  is the strain energy;  $C_{10}$ ,  $C_{20}$  and  $C_{30}$  are the expansion coefficients of the third-order reduced polynomial;  $I_1$  is the first invariant of strain.

Table 1. Reinforcement material properties.

Rebar material	Young's modulus (MPa)	Poisson's ratio ( $\mu$ )	Density (kg/m <sup>3</sup> )	Cord Angle (°)
Belt steel wire 1	105900	0.29	7800	66
Belt steel wire 2	105900	0.29	7800	114
Carcass cords	5250	0.3	1350	0

#### B. Finite Element Model

##### 1. Longitudinal Groove Tire Model

Using AutoCAD to draw the tire cross-section map. Because of the structural symmetry of the longitudinal groove pattern, only half of the outline sketch needs to be established, and the cross-section is drawn using the mirror image function. The sketch file is exported in DXF format, the DXF format file is converted into ig2 format entity model by using CATIA, and imported into Hypermesh.

The number and quality of grids directly affect the convergence, computation time and accuracy of the simulation results in the later stage [12]. Due to the special approximate incompressibility of tire rubber materials, hybrid elements are used for simulation in nonlinear finite element analysis. The 2D model meshing by Hypermesh software is shown in Fig. 2, and the model includes 939 nodes and 860 units. In the 2D plane finite element model, the triangular element type is CGAX3H, the quadrilateral element type is CGAX4H, and the rebar element type is SFMGAX1.

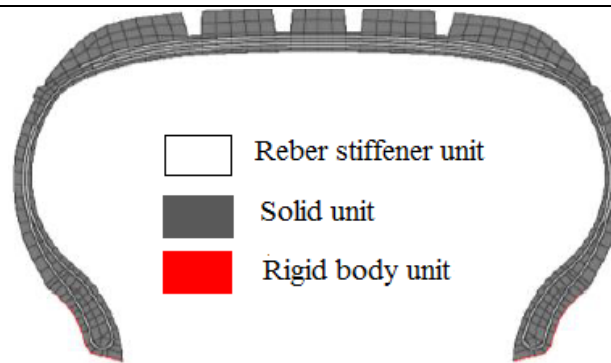


Fig. 2. Tire 2D mesh model.

The tire 2D grid model was output as 205.inp file, and the 3D solid grid was obtained by rotating the grid model with the keyword REVOLVE of ABAQUS. The contents of the keyword file were written as follows:

```
*SYMMETRIC MODEL GENERATION, REVOLVE, ELEMENT = 10000,
NODE = 10000, TRANSPORT
0.0, 0.0, 0.0, 0.0, 1.0, 0.0
0.0, 0.0, 1.0
360, 120,
```

After rotation, the 3d model has 197162 nodes and 110042 elements. Triangular element CGAX3H after rotation is 6-node pentahedral element C3D6, quadrilateral element CGAX4H after rotation is 8-node hexahedral element C3D8H, 2D Rebar element SFMCAX1 after rotation is 4-node tetrahedral surface element SFM3D4R. Rim and pavement are defined as analytic rigid bodies. The 3D longitudinal groove tire model meshing by Hypermesh software is shown in Fig. 3.



Fig. 3. 3D finite element model of longitudinal groove tire.

## 2. Complex Tread Patterns Tire Model

For complex tread patterns tires, a simulation model is established by using a combination model method, and the carcass part and the tread patterns part are separately modeled. Due to the complexity of connection between master node and slave node, the surface-to-surface contact connection must be adopted to improve the accuracy of contact stress between contact pairs and reduce the surface penetration [13].

The carcass modeling method is similar to the longitudinal groove tire modeling method. The 2D sketch is imported into the finite element software for grid division, and each part of the tire is given material and element type definition. The key word REVOLVE of ABAQUS is used to rotate the grid model to obtain the 3D solid grid. For tread patterns modeling. Firstly, CATIA software is used to build the solid model of the 3D pattern blocks. Furthermore, the 3D model is imported into Hypermesh software for positioning, creating contact surfaces and meshing. The mesh size is smaller than that of the carcass unit. After the modeling of carcass and tread patterns are completed, TIE command is used to bind and constrain the contact surface nodes of both.

This paper mainly introduces two binding constraint methods for tires with complex pattern block: (a) First create a tread patterns with a tread pitch, then, the tire carcass part and tread patterns part are bound together by binding command. Which require the block model and the carcass model to have good consistency in rotation angle, so as to ensure that the two can be completely attached. Use the keyword REVOLVE to rotate the above model to get a complete tire model. The modeling process is shown in Fig. 4(a). (b) The 3D tread patterns model is imported into Hypermesh software and meshed, and then the tread patterns with one pitch is rotated for one circle in the circumferential direction to obtain the complete tread patterns finite element model. Similarly, the carcass mesh model is circumferentially rotated to obtain a 3D solid mesh. Use binding commands to bind together, and the modeling process is shown in Fig. 4(b).

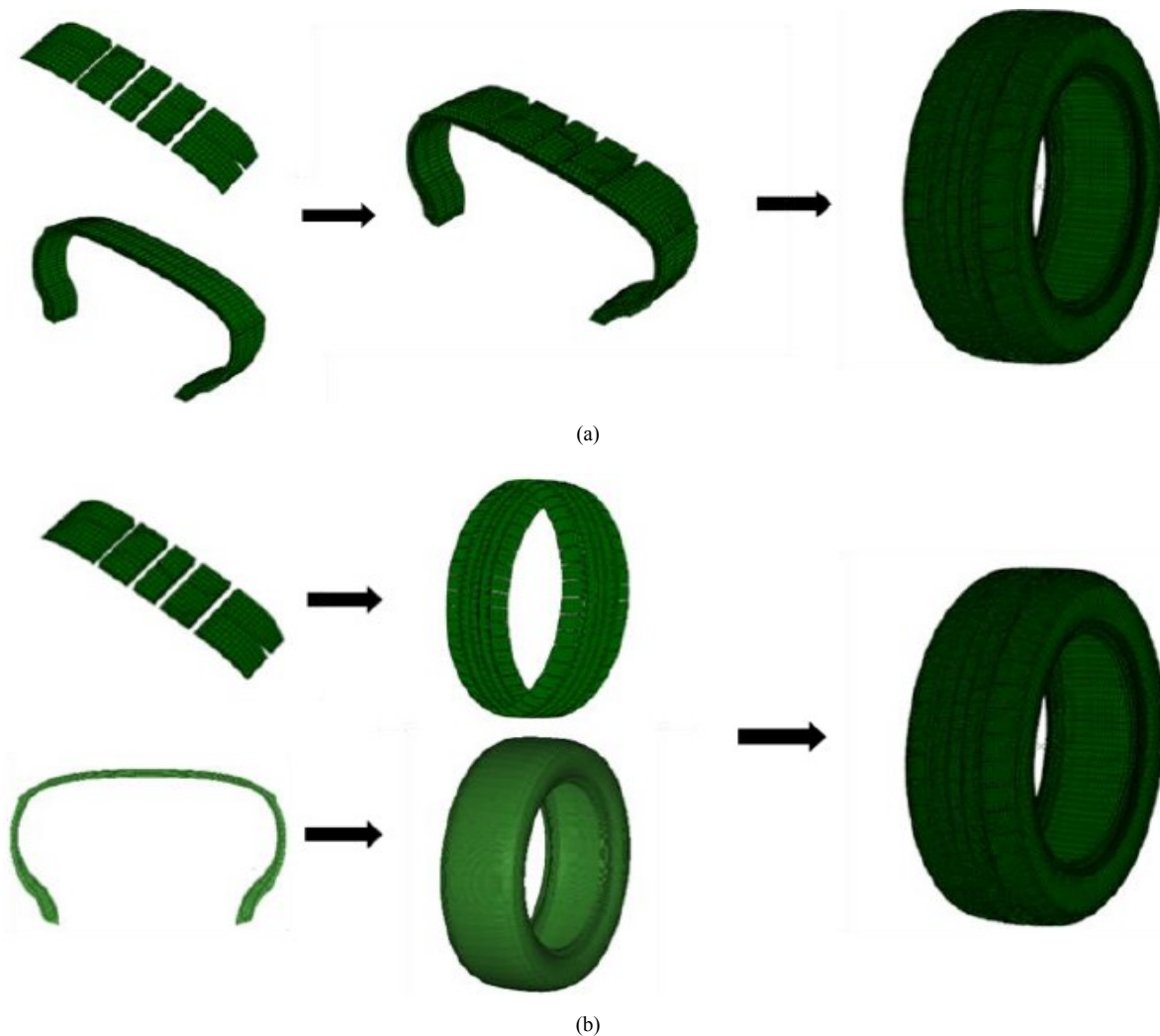


Fig. 4. Modeling process of complex tread tire.



The above two tire binding constraint methods has 307262 nodes and 171992 elements. Compared with the two methods, method (b) completes circumferential replication and rotation in the finite element software. In ABAQUS software, only TIE binding constraints are required to perform the next inflating and loading simulation, which reduce the computation time of simulation.

### C. Model Validation

In this paper, the static loading test was carried out on the tire, and the tire pressure was 2.6 bar during the analysis. The test verifies the validity of the model from radial deformation and contact patch respectively.

The comparison between the test and simulation results of the load-subsidence curve under static load is simulated by Origin software, as shown in Fig. 5. Where the slope of the curve can approximately represent the vertical stiffness of the tire under static load. The radial deformation of tire increases with the increase of load. Due to the material characteristics of rubber, the tire stiffness is small under small load. As the load increases, the stiffness tends to be constant, and the relationship between the two variables is approximately a linear function.

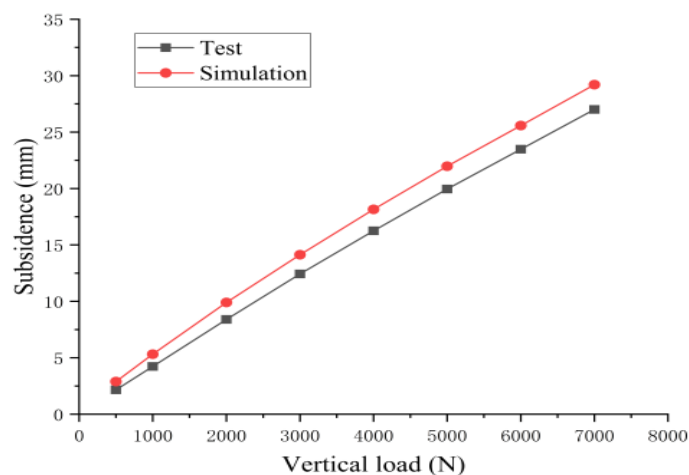


Fig. 5. Load - subsidence curve.

The comparison of the test and the simulated contact patch of the tire with complex tread patterns under static load is shown in Fig. 6, and the pressure distribution of the test and the simulated plot under the same load and pressure has good consistency. The comparison between the test and simulation values are shown in Table 2. The long axis length, short axis length and area of contact patch have small relative errors, with the maximum error being 5.3%, which is within the allowable range of engineering errors. Therefore, the tire simulation model made in this paper is reliable and can be used for finite element comparative analysis of complex tread patterns tires and longitudinal groove tires.

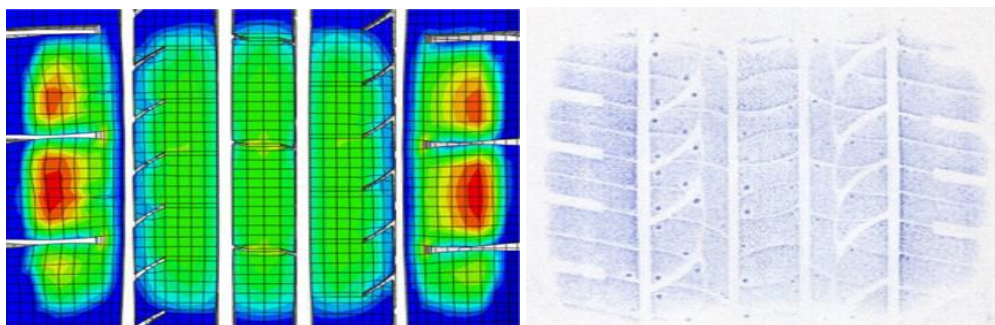


Fig. 6. Contact patch shape under static load.

Table 2. Comparison of contact patch test and simulation results.

Project	Test	Simulation	Relative error /%
Long axis length of contact patch /mm	128.45	132.19	2.9
Short axis length of contact patch /mm	101.20	103.64	2.4
Grounding area /mm <sup>2</sup>	13000	13700	5.3

#### IV. RESULTS AND DISCUSSION

##### A. Vertical Stress Distribution

The vertical stress distribution on the tread has an important influence on the wear resistance, durability and service life of the tire. The vertical stress distribution of longitudinal groove tire and complex tread patterns tire under different loads along the horizontal axis of grounding and the longitudinal axis of grounding are simulated by Origin software, as shown in Fig. 7 and Fig. 8.

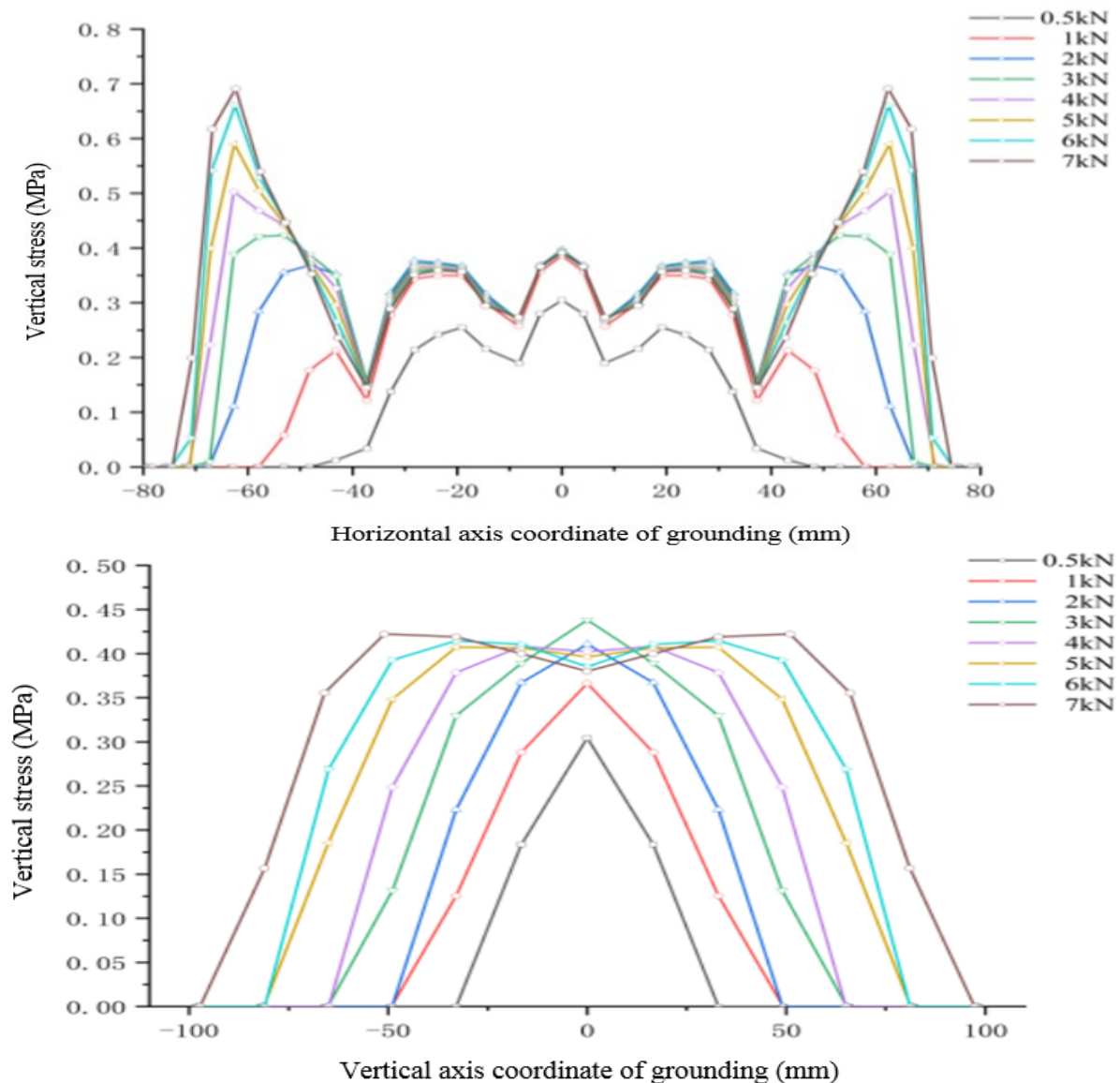


Fig. 7. Vertical Stress Distribution of Longitudinal Grooved Tire.

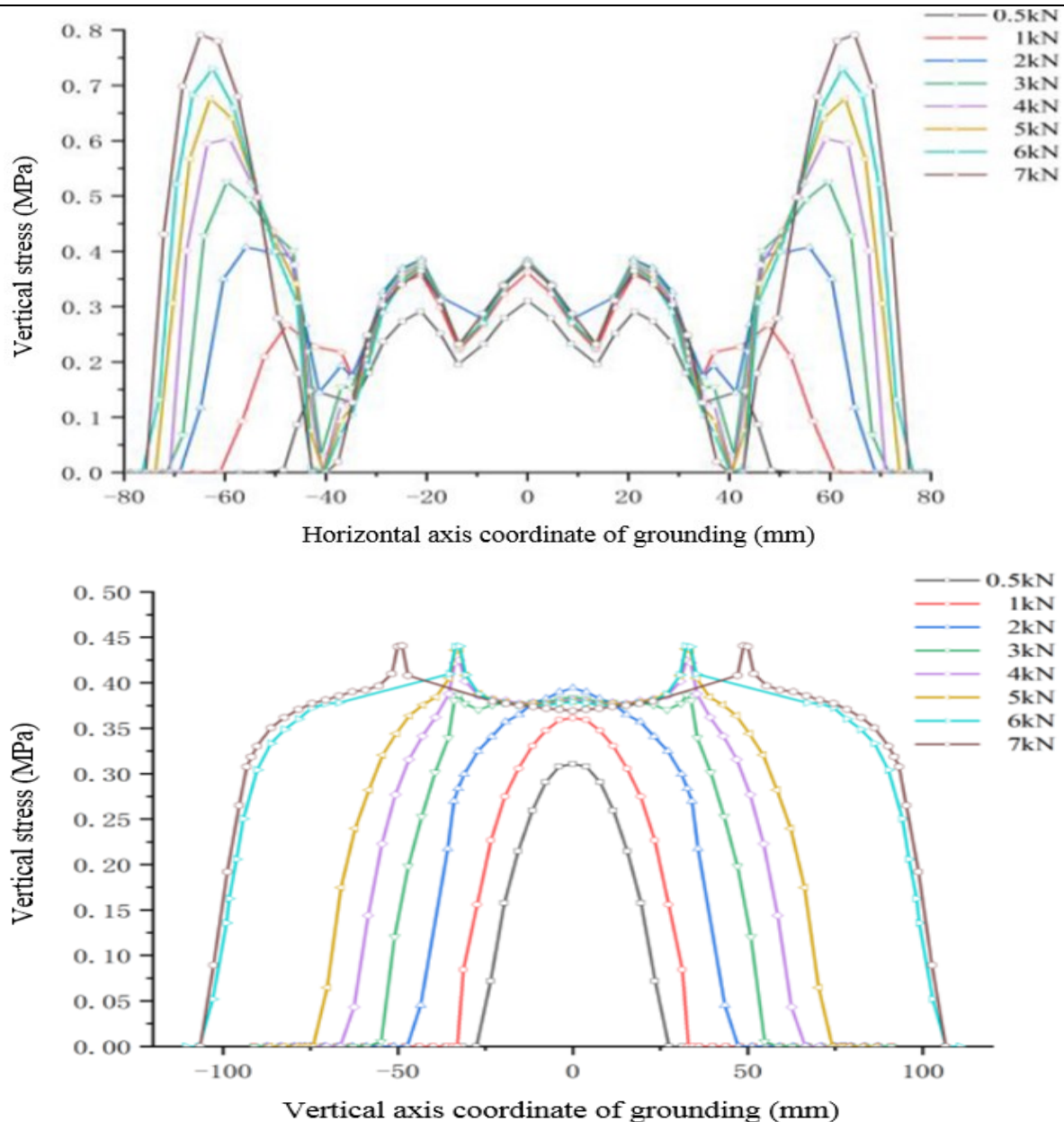


Fig. 8. Vertical Stress Distribution of Complex Tread Patterns Tire.

It can be seen from the figure that the vertical stress is mainly concentrated at the center of the crown when the load is small in the horizontal axis direction of grounding. With the increase of the load, the vertical stress gradually increases and the maximum vertical stress moves from the center location to the shoulder on both sides. This trend will lead to excessive deformation at the shoulder on both sides, and the temperature rise will increase correspondingly, causing shoulder damage and reducing the service life of the tire. In the direction of the grounding longitudinal axis, when the load is small, the vertical stress is mainly concentrated in the tire grounding center. With the increase of the load, the tread stress gradually increases, and the increase of the edge stress is larger than that of the grounding center, resulting in "warping phenomenon".

Compared with the vertical stress of longitudinal groove tire and complex tread patterns tire, it can be seen that the vertical stress of the two tires has little difference at small load. With the increase of load, the vertical stress at the horizontal axis grounding center under each load is approximately the same for the two types of tread patterns tires, but the vertical stress at the shoulder of complex tread patterns tire is greater than that of longitudinal



groove tire. In addition, comparing the vertical stress of the grounding longitudinal axis of Fig. 6 and Fig. 7, it can be seen that there is a small range of "stress mutation" and "warping phenomenon" is weakened. The reason is that there is stress concentration at the fine pattern in the complex tread patterns tires.

### B. Contact Patch Phenomenon

Tire is a double curvature rubber shell with curvature in both circumferential and transverse directions. Tire contact patch are closely related to various tire performances (traction, contact noise, driving smoothness and abrasion). Under the same tire pressure and different loads, the contact patch of some longitudinal groove tires and complex tread patterns tires are simulated by Abaqus software, as shown in Fig. 9. Under small load, the shape of the contact patch of the two tires is oval. With the increase of load, the shape of the contact patch changes from oval to rectangular, and the pressure peak location moves from the grounding center to the shoulder. Under different load conditions, the peak pressure of complex tread patterns tire is always greater than that of longitudinal tread tire, and the contact patch of longitudinal tread tire is distributed symmetrically about the horizontal axis of grounding.

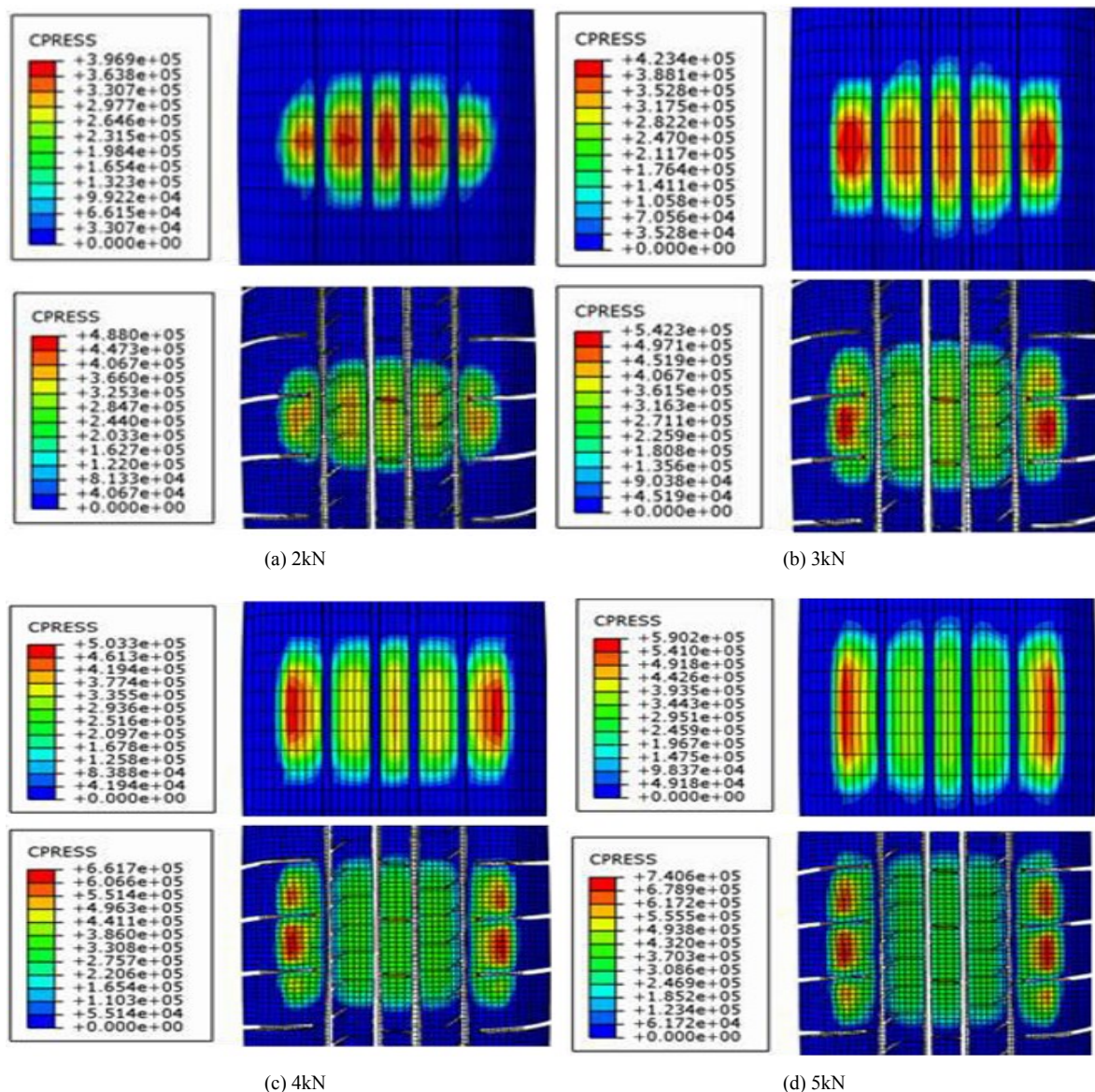


Fig. 9. Contact patch of two tires under different loads.

As shown in Fig. 10, the histogram of the change of the grounding area with the load shows that the tire grounding area increases nearly linearly with the increase of the load. Under different loads, the grounding area of tire with complex tread patterns is smaller than longitudinal groove tire. The reason is that compared with the longitudinal groove tire, the complex tread patterns tire has shoulder grooves and other pattern grooves, which leads to the reduction of the effective grounding area of the tire. This is also the main reason why the peak pressure of complex tread patterns tire is always greater than longitudinal groove tire.

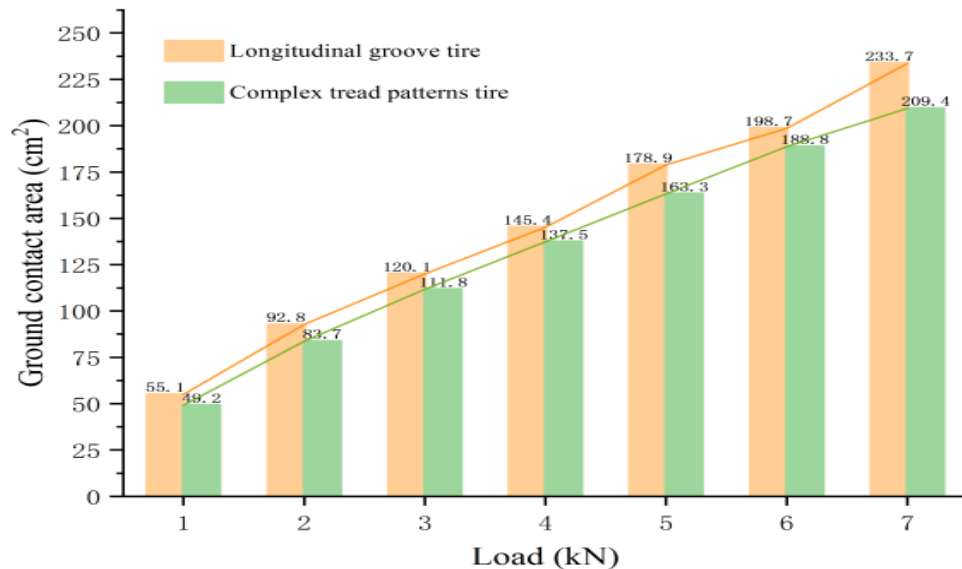


Fig. 10. Grounding area of two kinds of tires under different loads.

## V. CONCLUSION

In this paper, 205/55R16 longitudinal groove tire and complex tread patterns tire models are established. The correctness of the finite element model is verified by static loading tests. The load- subsidence curve, vertical stress distribution and contact patch of longitudinal groove tire and complex tread patterns tire are studied, the conclusion is as follows:

1. Firstly, with the increase of load, the radial deformation of tire increases gradually. At the initial stage of loading, due to the material characteristics of rubber, the tire stiffness is relatively small. As the load increases, the material is approximately incompressible and the stiffness tends to be constant.
2. Secondly, when the load is small, the vertical stress in the horizontal axis direction of the two tread patterns is mainly concentrated in the center of the tread. With the increase of the load, the vertical stress gradually increases and the maximum vertical stress moves from the center of crown to the shoulders on both sides. In the direction of the grounding longitudinal axis, the vertical stress is mainly concentrated in the tire grounding center. With the increase of load, the increase of edge stress is larger than that of the grounding center, resulting in "warping phenomenon". The increase of shoulder stress of complex tread patterns tire is larger than that of longitudinal groove tire.
3. Finally, With the increase of load, the shape of the contact patch changes from oval to rectangular, and the tire ground area gradually increases. Under various loads, the grounding area of complex tread patterns tires is smaller than longitudinal groove tires, and the stress peak value is increased compared with longitudinal groove tires, which is the reason why complex tread patterns are more prone to wear.

## REFERENCES

- [1] Alan N. Gent, Joseph D. Walter, Yintao Wei, et al, the Pneumatic Tire. Beijing: Tsinghua University Press, 2012.
- [2] Gang Cheng, Guoqun Zhao. The finite element analysis theory and application in radial tire. Beijing: Chemical Industry Press, 2015.
- [3] Akbar M. Farahani, Mohammad Mahjoob. Modal Analysis of a Non-rotating Inflated Tire using Experimental and Numerical Methods. International Journal of Engineering Innovation & Research, 7(1), 2018, pp. 15-21.
- [4] Koehne, S.H., B. Matute, and R. Mundl. Evaluation of Tire Tread and Body Interactions in the Contact Patch. Tire Science & Technology, 31(3), 2003, pp. 159-172.
- [5] HA. Si-ba-gen, Ling Zhu, Qin Shi, et al. Journal of Hefei University of Technology (Natural Science), 38(07), 2015, pp. 944-948.
- [6] Pillai P.S., Fielding-Russell G.S. Empirical Equations for Tire Footprint Area. Rubber Chemistry & Technology, 59(1), 1986, pp. 155-159.
- [7] Haibo Huang, Xudong Yu, Jinpeng Liu, et al, Asymmetry Investigation on Radial Tire Contact Pressure Distribution. Journal of System Simulation, 30(08), 2018, pp.180-187.
- [8] Hairong Chen, Guolin Wang. Finite Element Modeling Method of Radial Tire with Complex Pattern. China Rubber Industry, (05), 2012, pp. 40-43.
- [9] Huilin Du, Zhibin Gao. Finite Element Analysis of Motor Tyres. Automobile Parts, (04), 2018, pp. 11-15.
- [10] Zhen Yao. Modeling and contact features investigation of radial tire utilizing ABAQUS. Ningbo: Ningbo University, 2015.
- [11] Jun Wang, Liang Li, Lin Sun, et al, Finite Element Analysis of 245/70R16 Tire. Tire Industry, 36(9), 2016, pp. 502-528.
- [12] Zheng Yan, Marc 2001 from Beginner to Proficient. Beijing: China Water & Power Press, 2003, pp. 92-93.
- [13] Cho J.R., Kim K.W., Yoo W.S., et al. Mesh generation considering detailed tread blocks for reliable 3D tire analysis. Advances in Engineering Software, 35(2), 2004, pp. 105-113.

## AUTHOR'S PROFILE



### First Author

**Yongqiang Li**, Male, School of Transportation and Vehicle Engineering, Master in reading, Shandong University of Technology, 255049, Zhangdian district, Zibo city, Shandong province, China. email id: lyq961210@163.com



### Second Author

**Congzhen Liu**, Male, Associate professor, Doctor of Engineering, School of Transportation and Vehicle Engineering, Shandong University of Technology, 255049, Zhangdian district, Zibo city, Shandong province, China. email id: lcz200811@163.com



### Third Author

**Yunfen Sun**, Female, Master in reading, School of Transportation and Vehicle Engineering, Shandong University of Technology, 255049, Zhangdian district, Zibo city, Shandong province, China.



### Fourth Author

**Yalong Li**, Male, Master in reading, School of Transportation and Vehicle Engineering, Shandong University of Technology, 255049, Zhangdian district, Zibo city, Shandong province, China.



### Fifth Author

**Chengwei Xu**, Male, Master in reading, School of Transportation and Vehicle Engineering, Shandong University of Technology, 255049, Zhangdian district, Zibo city, Shandong province, China.



### Sixth Author

**Mengyu Xie**, Male, Master in reading, School of Transportation and Vehicle Engineering, Shandong University of Technology, 255049, Zhangdian district, Zibo city, Shandong province, China.